FERMILAB-PUB-15-002-T
ACCEPTED

Predicting positive parity B_s mesons from lattice QCD

C. B. Lang[a], Daniel Mohler[b], Sasa Prelovsek[c,d], R. M. Woloshyn[e]

[a]*Institute of Physics, University of Graz, A–8010 Graz, Austria*
[b]*Fermi National Accelerator Laboratory, Batavia, Illinois 60510-5011, USA*
[c]*Department of Physics, University of Ljubljana, 1000 Ljubljana, Slovenia*
[d]*Jozef Stefan Institute, 1000 Ljubljana, Slovenia*
[e]*TRIUMF, 4004 Wesbrook Mall Vancouver, BC V6T 2A3, Canada*

Abstract

We determine the spectrum of B_s 1P states using lattice QCD. For the $B_{s1}(5830)$ and $B^*_{s2}(5840)$ mesons, the results are in good agreement with the experimental values. Two further mesons are expected in the quantum channels $J^P = 0^+$ and 1^+ near the BK and B^*K thresholds. A combination of quark-antiquark and $B^{(*)}$ meson-Kaon interpolating fields are used to determine the mass of two QCD bound states below the $B^{(*)}K$ threshold, with the assumption that mixing with $B_s^{(*)}\eta$ and isospin-violating decays to $B_s^{(*)}\pi$ are negligible. We predict a $J^P = 0^+$ bound state B_{s0} with mass $m_{B_{s0}} = 5.711(13)(19)$ GeV. With further assumptions motivated theoretically by the heavy quark limit, a bound state with $m_{B_{s1}} = 5.750(17)(19)$ GeV is predicted in the $J^P = 1^+$ channel. The results from our first principles calculation are compared to previous model-based estimates.

Keywords:
hadron spectroscopy, lattice QCD, bottom-strange mesons
PACS: 11.15.Ha, 12.38.Gc

Over the years experiments have uncovered a number of mesons involving heavy quarks that do not seem to fit the simple quark-antiquark picture suggested by quark models. Examples of these include states in the charmonium and bottomonium spectrum [1] as well as the charm-strange $D^*_{s0}(2317)$ and $D_{s1}(2460)$ [2]. The latter states are identified with the $j = \frac{1}{2}$ heavy-quark multiplet, where j is the total angular momentum of the light quark [3]. These were predicted to be broad states above thresholds in potential models [4, 5, 6, 7]. However, the observed $D^*_{s0}(2317)$ and $D_{s1}(2460)$ are narrow states below the DK or D^*K thresholds [2], and it has been suggested that the thresholds play an important role in lowering the mass of the physical states [8]. In a recent lattice QCD simulation [9, 10, 11] these states are seen as QCD bound states below threshold with a mass in good agreement with experiment.

In the B_s meson spectrum only two positive parity states are known from experiment [12, 13, 14], the $B_{s1}(5830)$ and $B^*_{s2}(5840)$. The LHCb experiment should be able to see the remaining two states (0^+ and 1^+), which are expected to decay into s-wave states by emitting either a photon or a π^0 [15]. On the theory side there are a number of phenomenological model and EFT mass determinations [16, 17, 18, 19, 20, 21, 15, 5, 22, 23], a determination using Unitarized EFT based on low energy constants extracted from lattice QCD simulations [24], and some lattice QCD calculations in the static limit [25, 26, 27, 28, 29]. The HPQCD collaboration has published a prediction [30] taking into account explicitly only quark-antiquark operators and extracting only the ground states in the system. This strategy can lead to inaccurate results in the vicinity of thresholds where meson-meson scattering can have a significant effect. None of the previous lattice simulations clearly establish the states in question as either QCD bound states below threshold or resonances above threshold. It is this gap which we aim to fill with the current publication.

In this letter we present results for masses of the p-wave states of bottom-strange mesons with spin and parity quantum numbers $J^P = 0^+, 1^+, 2^+$. For the heavy-quark doublet with $j^P = \frac{3}{2}$ masses determined using only quark-antiquark operators agree with those of the observed $B_{s1}(5830)$ and $B^*_{s2}(5840)$. This, as well as calculated mass differences between heavy-light mesons, verifies our computational setup. Then we simulate $B^{(*)}K$ scattering in the scalar (axial) channel and extract the scattering matrix. Bound state poles are found below threshold and their location determines the masses of the B_{s0} and B_{s1}.

The gauge configurations are from the PACS-CS collaboration [31]. They have 2 + 1 flavors of dynamical quarks (up/down, strange); the bottom quark is implemented as a valence quark. The light and strange quarks are non-perturbatively improved Wilson fermions. The lattice spacing is 0.0907(13) fm and the Pion mass is 156(7)(2) MeV. The lattice size is $32^3 \times 64$ and we use stochastic distillation [32] for the quark propagation as in our analysis of the D_s mesons [9, 10, 11]. This allows to include contributions with annihilation diagrams. Further details including the u, d, and s quark parameters can be found in [10].

The dynamic strange quark mass and the associated hop-

Email addresses: `christian.lang@uni-graz.at` (C. B. Lang), `dmohler@fnal.gov` (Daniel Mohler), `sasa.prelovsek@ijs.si` (Sasa Prelovsek), `rwww@triumf.ca` (R. M. Woloshyn)

Operated by Fermi Research Alliance, LLC under Contract No. De-AC02-07CH11359 with the United States Department of Energy.

Table 1: Parameter values in the dispersion relation (1) for both the B and B^* meson in lattice units. For our uncertainty estimates we also use alternate parametrizations.

	B	B^*
M_1	1.5742(16)	1.5960(27)
M_2	2.16(29)	2.21(43)
M_4	1.4(2.6)	1.05(77)

ping parameter κ_s used in [31] differs significantly from the physical value. We therefore use a partially quenched strange quark $m_s^{val} \neq m_s^{sea}$. Different determinations agree very well and yield the value for κ_s[10] which leads to the Kaon mass $m_K = 504(1)(7)$ MeV.

The bottom quark is treated as a valence quark and the Fermilab method [33, 34] is used. See Ref. [35, 10] for details of our implementation. In the simplified form that we use [36, 37], only the bottom quark hopping parameter κ_b is tuned non-perturbatively, while the clover coefficients c_E and c_B are set to the tadpole improved value $c_E = c_B = c_{sw}^{(h)} = 1/u_0^3$, where u_0 denotes the average link. There are several ways of setting u_0 and we opt to use the Landau link on unsmeared gauge configurations. Within this simplified approach the static mass M_1 may have large discretization effects but mass differences are expected to be close to physical [38] and can be compared to experiment. Determining the bottom quark hopping parameter translates into determining the spin-averaged kinetic mass M_2 of 1S B_s mesons from the lattice dispersion relation [37]

$$E(p) = M_1 + \frac{\mathbf{p}^2}{2M_2} - \frac{a^3 W_4}{6}\sum_i p_i^4 - \frac{(\mathbf{p}^2)^2}{8M_4^3} + \ldots\,, \qquad (1)$$

where $\mathbf{p} = \frac{2\pi}{L}\mathbf{q}$ for a given spatial extent L. After trying multiple forms a simplified form without a W_4 term is taken[1] and for the value $\kappa_b = 0.096$ used in our simulation we obtain $M_{2,\overline{B_s}} = 5086(135)(73)$ MeV. This value is significantly smaller than the physical value $(m_{B_s} + 3m_{B_s^*})/4 = 5403.2^{+1.8}_{-1.6}$ MeV but the effects on the binding energies used in our analysis are small. This can be seen from the moderate difference between D_s [10] and B_s binding energies we obtain and will be accounted for in the systematic uncertainty. For the analysis of the phase shifts the dispersion relations for the Kaon (K) and the heavy meson (B or B^*) are needed. For the heavy B mesons we again take Eq. (1) with $W_4 = 0$ and the results are tabulated in Table 1. For the Kaon the relativistic dispersion relation $E_K(p) = \sqrt{m_K^2 + \mathbf{p}^2}$ is used.

The discrete energy levels for our combined basis of quark-antiquark and $B^{(*)}K$ operators are extracted from time correlations using the variational method [39, 40, 41, 42]. For a given

[1]The determination of the kinetic mass M_2 (including its uncertainty) and thereby what is identified with the "physical" meson mass is rather insensitive (i.e. varies by $\leq$ 15% of the uncertainty) to including or not including a W_4 term. (This is not the case for M_4 and its uncertainty.)

Table 2: Selected mass splittings (in MeV) of mesons involving bottom quarks compared to the values from the PDG [2]. A bar denotes spin average. Errors are statistical and scale-setting only.

Mass splitting	This work	Experiment
$m_{B^*} - m_B$	46.8(7.0)(0.7)	45.78(35)
$m_{B_{s^*}} - m_{B_s}$	47.1(1.5)(0.7)	$48.7^{+2.3}_{-2.1}$
$m_{B_s} - m_B$	81.5(4.1)(1.2)	87.35(23)
$m_\Upsilon - m_{\eta_b}$	44.2(0.3)(0.6)	62.3(3.2)
$2m_{\overline{B}} - m_{\overline{bb}}$	1190(11)(17)	1182.7(1.0)
$2m_{\overline{B_s}} - m_{\overline{bb}}$	1353(2)(19)	1361.7(3.4)
$2m_{B_c} - m_{\eta_b} - m_{\eta_c}$	169.4(0.4)(2.4)	167.3(4.9)

quantum channel one measures the Euclidean cross-correlation matrix $C_{ij}(t) = \langle O_i(t) O_j^\dagger(0)\rangle$ between several operators living on the corresponding time slices. The generalized eigenvalue problem disentangles the eigenstates $|n\rangle$. From the exponential decay of the eigenvalues $\lambda_n(t) \sim \exp(-E_n(t-t_0))$ one determines the energy values E_n of the eigenstates by exponential fits to the asymptotic behavior. The overlap factors $\langle O_i|n\rangle$ give the composition of the eigenstates in terms of the lattice operators. In order to obtain the lowest energy eigenstates and energy levels reliably one needs a sufficiently large set of operators with the chosen quantum numbers. All error values come from a jack-knife analysis, where the error analysis for the phase shift includes also the input from the dispersion relation (1).

To test our heavy quark approach we calculate a number of mass splittings involving heavy-light and/or heavy-heavy mesons, see Table 2. The quoted uncertainties are statistical and from scale-setting only and the values are not intended to be precision results. In particular our lighter than physical bottom quark mass strongly affects the spin-dependent splittings, but the effect tends to cancel with discretization errors. Estimates for both sources of uncertainty will be taken into account in our prediction of B_s mesons.

Partial wave unitarity implies that the scattering amplitude $T(s)$ for elastic $B^{(*)}K$ scattering can be written as

$$\sqrt{s}\,T^{-1}(s) = p\cot\delta(s) - \mathrm{i}p\,, \qquad (2)$$

where $p(s)$ is the momentum and $s = E^2$ the energy squared in the center of momentum system. Assuming a localized interaction region smaller than the spatial lattice extent a relation between the energy spectrum of meson-meson correlators in finite volume and the infinite volume phase shift δ has been derived [40, 43, 44, 45, 46],

$$f(p) \equiv p\cot\delta(p) = \frac{2\mathcal{Z}_{00}(1;(\frac{pL}{2\pi})^2)}{L\sqrt{\pi}} \approx \frac{1}{a_0} + \frac{1}{2}r_0 p^2\,, \qquad (3)$$

which applies in the elastic region and in the rest frame. $\mathcal{Z}_{00}$ denotes the generalized zeta function [44, 45] This real function $f(p)$ has no threshold singularity and the measured values can be found indeed above and below threshold. For s-wave

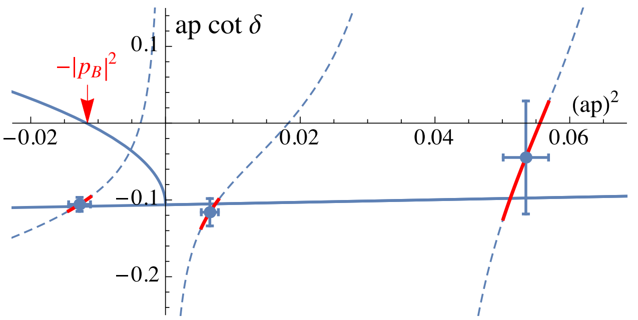

Figure 1: Plot of $ap\cot\delta(p)$ vs. $(ap)^2$ for BK scattering in s-wave. Circles are values from our simulation; red lines indicate the error band following the Lüscher curves (broken lines). The full line gives the linear fit (3) to the points. Below threshold $|p|$ is added and the zero of the combination (4) indicates the bound state position in infinite volume. Displayed uncertainties are statistical only.

scattering an effective range approximation (see Eq. (3)) may be used to interpolate between the closest points near threshold. The imaginary contribution to T^{-1} becomes real below threshold (responsible for a cusp in Re T). When the two contributions cancel, T^{-1} (see Eq. (2)) develops a zero where

$$f(\mathrm{i}|p_B|) + |p_B| = 0 \; . \tag{4}$$

That zero below threshold corresponds to a bound state pole of T in the upper Riemann sheet.

For $J^P = 0^+$ we computed cross-correlations between four $\bar{s}b$ (in the form given in Table XIII of [10]) and three BK (irreducible representation A_1^+) operators:

$$\begin{aligned} O_5 \equiv O_1^{BK} &= [\bar{s}\gamma_5 u]\,(\vec{p}=0)\,[\bar{u}\gamma_5 b]\,(\vec{p}=0) + \{u \to d\} \; , \\ O_6 \equiv O_2^{BK} &= [\bar{s}\gamma_t\gamma_5 u]\,(\vec{p}=0)\,[\bar{u}\gamma_t\gamma_5 b]\,(\vec{p}=0) + \{u \to d\} \; , \\ O_7 \equiv O_3^{BK} &= \sum_{\vec{p}=\pm e_{x,y,z}\,2\pi/L} [\bar{s}\gamma_5 u]\,(\vec{p})\,[\bar{u}\gamma_5 b]\,(-\vec{p}) + \{u \to d\} \; , \end{aligned} \tag{5}$$

where we assume that the closeness of the $BK\pi$ threshold can be ignored for our simulation. All operators are built according to the distillation method from quark sources that are eigenvectors of the spatial Laplacian, providing a smearing with a Gaussian-like envelope. The gauge links are four-dimensional normalized hypercubic (nHYP) smeared [47].

We omit $B_s^{(*)}\pi$ interpolators since we work in the isospin limit where such decays cannot occur. We also neglect $B_s^{(*)}\eta$, partially motivated by the threshold lying $\mathcal{O}(140$ MeV) above the $B^{(*)}K$ threshold. Inclusion would necessitate a coupled channel study which would need several volumes and considerably complicate the calculation.

As in earlier experience it turned out that the full set of operators gave noisier signals than suitable subsets so for the final analysis we use the operator set (1,2,4,5,7). The energy values resulting from correlated 2-exponential fits to the eigenvalues are given in Table 3.

In this channel B and K are in s-wave. If there is a bound state one expects an eigenstate with energy approaching the bound state energy from below in the infinite volume limit. The levels above threshold then would be dominated by BK operators with back-to-back momenta. This is exactly what is seen from the overlap ratios: The lowest level is dominated by operators 1,2 and 4, level 2 by the $B(0)K(0)$ operator 5 and level 3 by the $B(1)K(-1)$ operator 7.

As shown in (3) we can use the values of $p\cot\delta(p)$ from Lüscher's relation to determine the effective range parametrization near threshold. The energy eigenvalues give the points shown in Fig. 1 together with a linear fit. The value and slope at threshold can be related to the scattering length and effective range:

$$a_0^{BK} = -0.85(10)\,\mathrm{fm} \; , \qquad r_0^{BK} = 0.03(15)\,\mathrm{fm} \; . \tag{6}$$

Equation (4) gives the bound state position. From this the binding energy is estimated to be $m_B + m_K - m_{B_{s0}} = 64(13)(19)$ MeV; thus, using the physical threshold as input to minimize systematic effects, we predict a bound state B_{s0} with $J^P = 0^+$ at a mass of

$$m_{B_{s0}} = 5.711(13)(19)\,\mathrm{GeV} \; . \tag{7}$$

The first error is due to statistics and the effective range fit, and the second value is our estimate for the systematic error with the main contributions due to heavy quark discretization, unphysical Kaon mass, and finite volume effects. Details of this uncertainty estimate are provided in Table 4.

Table 4: Systematic uncertainties in the mass determination of the below-threshold states with quantum numbers $J^P = 0^+, 1^+$. The heavy-quark discretization effects are quantified by calculating the Fermilab-method mass mismatches and employing HQET power counting [34] with $\Lambda = 700$ MeV. The dominant contributions arise from mismatches in m_B and m_E and their size as a fraction of the reference scale Λ can be seen in Fig. 3 of [34]. The finite volume uncertainties are estimated conservatively by the difference of the lowest energy level and the pole position (see also Equations (9) and (28) of [48]). The last line gives the effect of using only the two points near threshold for the effective range fit. The third point might be affected more strongly by the $B_s^{(*)}\eta$ threshold, so it is reassuring that the difference in results between two-point and three-point fits is minimal. The total uncertainty has been obtained by adding the single contributions in quadrature.

source of uncertainty	expected size [MeV]
heavy-quark discretization	12
finite volume effects	8
unphysical Kaon, isospin & EM	11
b-quark tuning	3
dispersion relation	2
spin-average (experiment)	2
scale uncertainty	1
3 pt vs. 2 pt linear fit	2
total	19

For $J^P = 1^+$ we computed cross-correlations between eight $\bar{s}b$ (in the form given in Table XIII of [10]) and three B^*K (irrep

Table 3: Energy levels for $J^P = 0^+$ (upper set), 1^+ (middle set) and 2^+ (lower set). A correlated 2-exponential fit is used and $\overline{m} = \frac{1}{4}(m_{B_s} + 3m_{B_s^*})$ with $\overline{m} = 1.62897(43)$ in lattice units. t_0 denotes the reference point in the generalized eigenvalue problem. Energy 2 in the middle set corresponds to the $B_{s1}^*(5830)$. The lower set shows the naive energy level for the $J^P = 2^+$ and corresponds to the $B_{s2}^*(5840)$ using the same operator basis used in [10] for the D_{s2}^*.

level	t_0	basis	fit range	$\frac{\chi^2}{d.o.f}$	Ea	$E - \overline{m}$ [GeV]	$(ap)^2$	$ap\ \cot(\delta)$	p^2[GeV^2]	$p\ \cot(\delta)$ [GeV]
1	2	$O_{1,2,4,5,7}$	4-16	0.53	1.7735 (44)	0.315 (9)	-0.0128 (19)	-0.106(10)	-0.0606(88)	-0.231(23)
2	2	$O_{1,2,4,5,7}$	4-16	1.05	1.8213 (29)	0.419 (6)	0.0066 (13)	-0.116(18)	0.0312(62)	-0.252(40)
3	2	$O_{1,2,4,5,7}$	3-13	1.35	1.9139 (59)	0.620 (13)	0.0535 (35)	-0.045(76)	0.2532(165)	-0.097(166)
1	2	$O_{3,4,6,9,11}$	4-14	0.67	1.7919 (51)	0.353 (11)	-0.0141(22)	-0.113(11)	-0.067(11)	-0.246(25)
2	2	$O_{3,4,6,9,11}$	3-14	0.85	1.8255 (42)	0.428 (9)	–	–	–	–
3	2	$O_{3,4,6,9,11}$	3-14	0.54	1.8395 (45)	0.457 (10)	0.0050(24)	-0.142(49)	0.024(11)	-0.308(106)
4	2	$O_{3,4,6,9,11}$	3-14	1.19	1.9406 (50)	0.677 (11)	0.0566(31)	0.021(67)	0.268(15)	0.046(145)
1	2	$O_{1,2}$	4-14	0.43	1.8357(51)	0.450 (11)	–	–	–	–

T_1^+) operators:

$$O_9 \equiv O_{1,k}^{B^*K} = [\bar{s}\gamma_5 u]\,(\vec{p}=0)\,[\bar{u}\gamma_k b]\,(\vec{p}=0) + \{u \to d\}\ ,$$
$$O_{10} \equiv O_{2,k}^{B^*K} = [\bar{s}\gamma_t\gamma_5 u]\,(\vec{p}=0)\,[\bar{u}\gamma_t\gamma_k b]\,(\vec{p}=0) + \{u \to d\}\ ,$$
$$O_{11} \equiv O_{3,k}^{B^*K} = \sum_{\vec{p}=\pm e_{x,y,z}\ 2\pi/L} [\bar{s}\gamma_5 u]\,(\vec{p})\,[\bar{u}\gamma_k b]\,(-\vec{p}) + \{u \to d\}\ .$$

Comparing various subsets of operators the most stable set was (3,4,6,9,11), where four energy levels could be determined (Table 3).

Based on the overlaps, levels 3 and 4 are dominated by operators 9 ($B^*(0)K(0)$) and 11 ($B^*(1)K(-1)$), respectively. The lowest energy level (dominated by operators 3 and 4) agrees with a bound state interpretation. A linear fit to the points corresponding to energy levels 1, 3 and 4 gives the scattering parameters

$$a_0^{B^*K} = -0.97(16)\,\text{fm}\ , \qquad r_0^{B^*K} = 0.28(15)\,\text{fm}\ . \tag{8}$$

This indicates a B^*K bound state B_{s1} with a binding energy of 71(17)(19) MeV. Using again the physical threshold as input we obtain

$$m_{B_{s1}} = 5.750(17)(19)\,\text{GeV}\ . \tag{9}$$

This state has not (yet) been observed in experiments.

Notice that our determination assumes that the effect of s-wave – d-wave mixing is negligible on the scale of our uncertainty. This is motivated theoretically by the heavy quark limit [3] (where such mixing is absent), which should be a good approximation for bottom-strange mesons.

Level 2 (dominated by operator 6) lies just below threshold. This is interpreted, as in the case of the $D_{s1}(2536)$ [10], to be the $j = \frac{3}{2}$ state with $J^P = 1^+$ which does not couple to B^*K in s-wave in the heavy quark limit [3]. The composition of the state with regard to the $\overline{q}q$ operators is fairly independent of whether the B^*K operators are included or not. Assuming that the coupling to B^*K in s-wave is indeed small, the "avoided level crossing" region is so narrow that this state may be treated as decoupled from the B^*K scattering channel. Taking the mass difference with respect to the B_s spin average and adding the physical value gives

$$m_{B'_{s1}} = 5.831(9)(6)\,\text{GeV}\ , \tag{10}$$

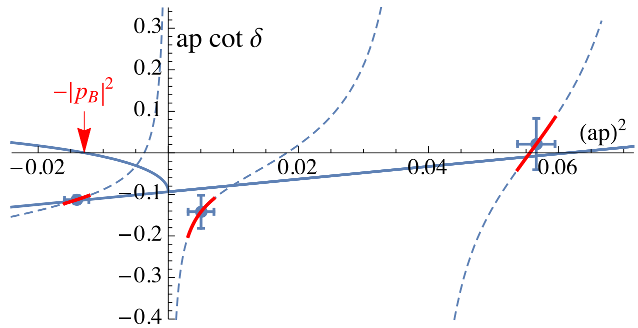

Figure 2: Plot of $ap\cot\delta(p)$ vs. $(ap)^2$ for B^*K scattering in s-wave, as given by the levels 1, 3 and 4 in Table 3; see analogous caption of Fig. 1.

where the errors are statistical and scale-setting only. In experiments [12, 14] one finds a resonance $B_{s1}(5830)$ decaying dominantly into $B^{*+}K^-$ 10 MeV above threshold at 5.8287(4) GeV. The masses are in excellent agreement.

The lowest energy level with $J^P = 2^+$ (irrep T_2^+) corresponding to the $B_{s2}^*(5840)$ is extracted using just $\bar{s}b$ operators. The resulting mass is

$$m_{B_{s2}} = 5.853(11)(6)\,\text{GeV}\ , \tag{11}$$

consistent with the observed value [2].

In summary we have analyzed the spectrum of positive parity B_s mesons[2] and find two bound states below threshold, corresponding to the as-yet-unobserved B_{s0}^* and B_{s1} 1P states. Table 5 compares our first-principles lattice QCD calculation to previous results. Different variants of Unitarized ChPT along with phenomenological or lattice input (in particular [19, 24]) lead to mass predictions that are in good agreement with our calculation. Also, the model based on heavy-quark and chiral symmetry by Bardeen, Eichten and Hill [15] gives results that are remarkably close.

[2]The binding energies of the corresponding D_s mesons were also reanalyzed with our updated procedure (basis, dispersion relation, etc.) and are fully compatible with our old results [35, 10] and, within systematic uncertainties, with experiment.

Table 5: Comparison of masses from this work to results from various model based calculations; all masses in MeV.

J^P	0^+	1^+
Covariant (U)ChPT [24]	5726(28)	5778(26)
NLO UHMChPT [19]	5696(20)(30)	5742(20)(30)
LO UChPT [17, 18]	5725(39)	5778(7)
LO χ-SU(3) [16]	5643	5690
HQET + ChPT [20]	5706.6(1.2)	5765.6(1.2)
Bardeen, Eichten, Hill [15]	5718(35)	5765(35)
rel. quark model [5]	5804	5842
rel. quark model [22]	5833	5865
rel. quark model [23]	5830	5858
HPQCD [30]	5752(16)(5)(25)	5806(15)(5)(25)
this work	5713(11)(19)	5750(17)(19)

Acknowledgements

We thank the PACS-CS collaboration for providing the gauge configurations. D. M. would like to thank E. Eichten, R. Van de Water and J. Simone for insightful discussions. The calculations were performed on computing clusters at the University of Graz (NAWI Graz) and with USQCD resources at Fermilab, supported by the DOE. This work is supported in part by the Austrian Science Fund (FWF):[I1313-N27], by the Slovenian Research Agency ARRS project N1-0020 and by the Natural Sciences and Engineering Research Council of Canada. Fermilab is operated by Fermi Research Alliance, LLC under Contract No. De-AC02-07CH11359 with the United States Department of Energy.

References

[1] N. Brambilla, et al., QCD and Strongly Coupled Gauge Theories: Challenges and Perspectives, Eur. Phys. J. C 74 (2014) 2981. arXiv:1404.3723.

[2] K. A. Olive, et al., Review of Particle Physics, Chin. Phys. C 38 (2014) 090001. doi:10.1088/1674-1137/38/9/090001.

[3] N. Isgur, M. B. Wise, Spectroscopy with heavy quark symmetry, Phys. Rev. Lett. 66 (1991) 1130. doi:10.1103/PhysRevLett.66.1130.

[4] S. Godfrey, R. Kokoski, The Properties of p Wave Mesons with One Heavy Quark, Phys. Rev. D 43 (1991) 1679. doi:10.1103/PhysRevD.43.1679.

[5] M. Di Pierro, E. Eichten, Excited heavy - light systems and hadronic transitions, Phys. Rev. D 64 (2001) 114004. arXiv:hep-ph/0104208, doi:10.1103/PhysRevD.64.114004.

[6] S. Godfrey, N. Isgur, Mesons in a Relativized Quark Model with Chromodynamics, Phys. Rev. D 32 (1985) 189–231. doi:10.1103/PhysRevD.32.189.

[7] D. Ebert, V. Galkin, R. Faustov, Mass spectrum of orbitally and radially excited heavy - light mesons in the relativistic quark model, Phys. Rev. D 57 (1998) 5663–5669. arXiv:hep-ph/9712318, doi:10.1103/PhysRevD.59.019902,10.1103/PhysRevD.57.5663.

[8] E. van Beveren, G. Rupp, Observed $D_s(2317)$ and tentative D(2030) as the charmed cousins of the light scalar nonet, Phys. Rev. Lett. 91 (2003) 012003. arXiv:hep-ph/0305035, doi:10.1103/PhysRevLett.91.012003.

[9] D. Mohler, C. B. Lang, L. Leskovec, S. Prelovsek, R. M. Woloshyn, $D_{s0}^*(2317)$ Meson and D-Meson Kaon Scattering from Lattice QCD, Phys. Rev. Lett. 111 (2013) 222001. arXiv:1308.3175.

[10] C. B. Lang, L. Leskovec, D. Mohler, S. Prelovsek, R. M. Woloshyn, D_s mesons with DK and D^*K scattering near threshold, Phys. Rev. D 90 (2014) 034510. arXiv:1403.8103.

[11] C. B. Lang, L. Leskovec, D. Mohler, S. Prelovsek, R. M. Woloshyn, DK and D^*K scattering near threshold, PoS LATTICE2014 (2014) 086. arXiv:1410.6668.

[12] T. Aaltonen, et al., Observation of orbitally excited B_s mesons, Phys. Rev. Lett. 100 (2008) 082001. arXiv:0710.4199, doi:10.1103/PhysRevLett.100.082001.

[13] V. Abazov, et al., Observation and properties of the orbitally excited B*(s2) meson, Phys. Rev. Lett. 100 (2008) 082002. arXiv:0711.0319, doi:10.1103/PhysRevLett.100.082002.

[14] R. Aaij, et al., First observation of the decay $B_{s2}^*(5840)^0 \to B^{*+}K^-$ and studies of excited B_s^0 mesons, Phys. Rev. Lett. 110 (15) (2013) 151803. arXiv:1211.5994, doi:10.1103/PhysRevLett.110.151803.

[15] W. A. Bardeen, E. J. Eichten, C. T. Hill, Chiral multiplets of heavy - light mesons, Phys. Rev. D 68 (2003) 054024. arXiv:hep-ph/0305049, doi:10.1103/PhysRevD.68.054024.

[16] E. Kolomeitsev, M. Lutz, On Heavy light meson resonances and chiral symmetry, Phys. Lett. B 582 (2004) 39–48. arXiv:hep-ph/0307133, doi:10.1016/j.physletb.2003.10.118.

[17] F.-K. Guo, P.-N. Shen, H.-C. Chiang, R.-G. Ping, B.-S. Zou, Dynamically generated 0+ heavy mesons in a heavy chiral unitary approach, Phys. Lett. B 641 (2006) 278–285. arXiv:hep-ph/0603072, doi:10.1016/j.physletb.2006.08.064.

[18] F.-K. Guo, P.-N. Shen, H.-C. Chiang, Dynamically generated 1+ heavy mesons, Phys. Lett. B 647 (2007) 133–139. arXiv:hep-ph/0610008, doi:10.1016/j.physletb.2007.01.050.

[19] M. Cleven, F.-K. Guo, C. Hanhart, U.-G. Meissner, Light meson mass dependence of the positive parity heavy-strange mesons, Eur. Phys. J. A47 (2011) 19. arXiv:1009.3804, doi:10.1140/epja/i2011-11019-2.

[20] P. Colangelo, F. De Fazio, F. Giannuzzi, S. Nicotri, New meson spectroscopy with open charm and beauty, Phys. Rev. D 86 (2012) 054024. arXiv:1207.6940, doi:10.1103/PhysRevD.86.054024.

[21] H.-Y. Cheng, F.-S. Yu, Near mass degeneracy in the scalar meson sector: Implications for $B_{(s)0}^*$ and $B_{(s)1}'$ mesons, Phys. Rev. D 89 (11) (2014) 114017. arXiv:1404.3771, doi:10.1103/PhysRevD.89.114017.

[22] D. Ebert, R. Faustov, V. Galkin, Heavy-light meson spectroscopy and Regge trajectories in the relativistic quark model, Eur. Phys. J. C66 (2010) 197–206. arXiv:0910.5612, doi:10.1140/epjc/s10052-010-1233-6.

[23] Y. Sun, Q.-T. Song, D.-Y. Chen, X. Liu, S.-L. Zhu, Higher bottom and bottom-strange mesons, Phys. Rev. D 89 (2014) 054026. arXiv:1401.1595, doi:10.1103/PhysRevD.89.054026.

[24] M. Altenbuchinger, L. S. Geng, W. Weise, Scattering lengths of Nambu-Goldstone bosons off D mesons and dynamically generated heavy-light mesons, Phys. Rev. D 89 (2014) 014026. arXiv:1309.4743.

[25] C. McNeile, C. Michael, G. Thompson, Hadronic decay of a scalar B meson from the lattice, Phys. Rev. D 70 (2004) 054501. arXiv:hep-lat/0404010, doi:10.1103/PhysRevD.70.054501.

[26] J. Foley, A. O. Cais, M. Peardon, S. M. Ryan, Static-light mesons on a dynamical anisotropic lattice (2006). arXiv:hep-lat/0610062.

[27] J. Koponen, Energies of B_s meson excited states: A Lattice study, Phys. Rev. D 78 (2008) 074509. arXiv:0708.2807, doi:10.1103/PhysRevD.78.074509.

[28] T. Burch, C. Hagen, C. B. Lang, M. Limmer, A. Schäfer, Excitations of single-beauty hadrons, Phys. Rev. D 79 (2009) 014504. arXiv:0809.1103.

[29] C. Michael, A. Shindler, M. Wagner, The continuum limit of the static-light meson spectrum, JHEP 1008 (2010) 009. arXiv:1004.4235, doi:10.1007/JHEP08(2010)009.

[30] E. B. Gregory, C. T. Davies, I. D. Kendall, J. Koponen, K. Wong, et al., Precise B, B_s and B_c meson spectroscopy from full lattice QCD, Phys. Rev. D 83 (2011) 014506. arXiv:1010.3848, doi:10.1103/PhysRevD.83.014506.

[31] S. Aoki, K.-I. Ishikawa, N. Ishizuka, T. Izubuchi, D. Kadoh, K. Kanaya, Y. Kuramashi, Y. Namekawa, M. Okawa, Y. Taniguchi, A. Ukawa, N. Ukita, T. Yoshie, 2+1 Flavor Lattice QCD toward the Physical Point, Phys. Rev. D 79 (2009) 034503. arXiv:0807.1661.

[32] C. Morningstar, J. Bulava, J. Foley, K. J. Juge, D. Lenkner, M. Peardon, C. H. Wong, Improved stochastic estimation of quark propagation with Laplacian Heaviside smearing in lattice QCD, Phys. Rev. D 83 (2011) 114505. arXiv:1104.3870.

[33] A. X. El-Khadra, A. S. Kronfeld, P. B. Mackenzie, Massive

Fermions in Lattice Gauge Theory, Phys. Rev. D 55 (1997) 3933. arXiv:hep-lat/9604004, doi:10.1103/PhysRevD.55.3933.
[34] M. B. Oktay, A. S. Kronfeld, New lattice action for heavy quarks, Phys. Rev. D 78 (2008) 014504. arXiv:0803.0523, doi:10.1103/PhysRevD.78.014504.
[35] D. Mohler, S. Prelovsek, R. M. Woloshyn, D Pi scattering and D meson resonances from lattice QCD, Phys. Rev. D 87 (2013) 034501. arXiv:1208.4059.
[36] T. Burch, et al., Quarkonium mass splittings in three-flavor lattice QCD, Phys. Rev. D 81 (2010) 034508. arXiv:0912.2701, doi:10.1103/PhysRevD.81.034508.
[37] C. Bernard, et al., Tuning Fermilab Heavy Quarks in 2+1 Flavor Lattice QCD with Application to Hyperfine Splittings, Phys. Rev. D 83 (2011) 034503. arXiv:1003.1937, doi:10.1103/PhysRevD.83.034503.
[38] A. S. Kronfeld, Application of heavy quark effective theory to lattice QCD. 1. Power corrections, Phys.Rev. D62 (2000) 014505. arXiv:hep-lat/0002008, doi:10.1103/PhysRevD.62.014505.
[39] C. Michael, Adjoint Sources in Lattice Gauge Theory, Nucl. Phys. B 259 (1985) 58. doi:10.1016/0550-3213(85)90297-4.
[40] M. Lüscher, Volume dependence of the energy spectrum in massive quantum field theories. I. Stable particle states, Commun. Math. Phys. 104 (1986) 177. doi:10.1007/BF01211589.
[41] M. Lüscher, U. Wolff, How to calculate the Elastic Scattering Matrix in 2-Dimensional QuantumField Theories by Numerical Simulation, Nucl. Phys. B 339 (1990) 222.
[42] B. Blossier, M. Della-Morte, G. von Hippel, T. Mendes, R. Sommer, On the generalized eigenvalue method for energies and matrix elements in lattice field theory, JHEP 0904 (2009) 094. arXiv:0902.1265, doi:doi:10.1088/1126-6708/2009/04/094.
[43] M. Lüscher, Volume dependence of the energy spectrum in massive quantum field theories. II. Scattering states, Commun. Math. Phys. 105 (1986) 153. doi:10.1007/BF01211097.
[44] M. Lüscher, Two-Particle States on a Torus and Their Relation to the Scattering Matrix, Nucl. Phys. B 354 (1991) 531. doi:10.1016/0550-3213(91)90366-6.
[45] M. Lüscher, Signatures of unstable particles in finite volume, Nucl. Phys. B 364 (1991) 237. doi:10.1016/0550-3213(91)90584-K.
[46] R. A. Briceno, Two-particle multichannel systems in a finite volume with arbitrary spin, Phys. Rev. D 89 (2014) 074507. arXiv:1401.3312, doi:10.1103/PhysRevD.89.074507.
[47] A. Hasenfratz, R. Hoffmann, S. Schaefer, Hypercubic smeared links for dynamical fermions, JHEP 0705 (2007) 029. arXiv:hep-lat/0702028, doi:10.1088/1126-6708/2007/05/029.
[48] S. Sasaki, T. Yamazaki, Signatures of S-wave bound-state formation in finite volume, Phys. Rev. D 74 (2006) 114507. arXiv:hep-lat/0610081, doi:10.1103/PhysRevD.74.114507.